

The effect of chloride ions and organic matter on the photodegradation of acetamiprid in saline waters

M.I. Pinto^{a,b}, R. Salgado^{a,c}, C.A.T. Laia^a, William J. Cooper^d, G. Sontag^e, Hugh D. Burrows^f, L. Branco^a, C. Vale^b, J.P. Noronha^{a,*}

^a LAQV, REQUIMTE, Departamento de Química, Faculdade de Ciências e Tecnologia, Universidade NOVA de Lisboa, 2829-516, Caparica, Portugal

^b CIIMAR, Interdisciplinary Center of Marine and Environmental Research, Rua dos Bragas, n° 289, 4050-123, Porto, Portugal

^c ESTS-IPS-CINEA, Escola Superior de Tecnologia de Setúbal do Instituto Politécnico de Setúbal, Rua Vale de Chaves, Campus do IPS, Estefanilha, 2910-761, Setúbal, Portugal

^d University of California, Irvine, Department of Civil and Environmental Engineering, Irvine, CA, 92697-2175, USA

^e Institute for Analytical Chemistry, University of Vienna, Waehringerstr. 38, A-1090, Vienna, Austria

^f Centro de Química, Chemistry Department, University of Coimbra, 3004-535, Coimbra, Portugal

ARTICLE INFO

Keywords:

Pesticides
Neonicotinoids
Climate change
Salinity
DOM
Photolysis

ABSTRACT

The photodegradation kinetics of the neonicotinoid insecticide acetamiprid (ACT) was investigated under different conditions of pH, salinity and dissolved organic matter (DOM). Photodegradation of ACT in saline and freshwaters followed pseudo-first-order kinetics. Varying pH from 5 to 9 did not significantly affect the photodegradation rate constants (k_p) of ACT. Addition of chloride ions increased significantly the value of k_p . In the presence of AHA, 10 mg L⁻¹, k_p was reduced to approximately 34% of that in sodium chloride solutions 35 g L⁻¹. The observed inhibition may be a consequence of the antioxidant properties of DOM and/or the shading of DOM in the solution. In coastal waters, k_p showed a tendency to increase with increasing of salinity and to decrease in the presence of DOM. This is an important outcome since coastal lagoons are important and dynamic systems that are likely to be highly influenced by global climate changes.

1. Introduction

Acetamiprid (ACT) is a neonicotinoid insecticide (Fig. 1) applied for the control of a wide range of insects in crops such as vegetables, fruit trees, rice, wheat, etc. [1,2]. The compound belongs to a growing class of commercialized pesticides that has reached in the last years between 17 and 30% of the global pesticide market [2–5]. In spite of its growing application, the compound is toxic to birds, earthworms, honeybees and some aquatic organisms [1,6–8]. Because of its adverse effects, ACT has recently been added to the “watch list of substances” for European Union water monitoring under Decision 2015/495/EU [9]. The monitoring of such listed substances aims to generate high-quality data on their concentration in the aquatic environment fit for the purpose of supporting future prioritisation and risks assessments [9]. Findings relating to the behaviour of ACT in aquatic systems are, therefore, of considerable relevance.

In recent years several studies on the photodegradation of ACT have been presented [2,6,10–14]. The reactivity, mechanisms and primary degradation products of ACT with environmental occurring reactive species e.g. hydroxyl radical ($\cdot\text{OH}$), singlet oxygen ($^1\text{O}_2$), carbonate

radicals ($\cdot\text{CO}_3^-$) and excited triplet state of dissolved organic matter ($^3\text{DOM}^*$) have been reported in the literature [6,10–13]. Removal of ACT from different water matrix using advanced oxidation procedures (AOP) such as solar photo-Fenton and heterogeneous photocatalysis using UV-irradiated titanium oxide have also been studied [2,14,15]. However, to the best of our knowledge, the influence of chloride ions on the photodegradation of ACT in saline waters, with and without dissolved organic matter (DOM), has never been studied. DOM is a complex mixture of organic structures, which work either as sensitizer or an inhibitor of the photodegradation of pesticides and other pollutants, such as antibiotics [16–22]. A number of studies have revealed that chloride ions and other halides can also have a significant impact on photochemical activity of DOM and, consequently, on environmental fate of pesticides [23–25]. The lack of information concerning the photodegradation of ACT in saline waters is therefore an important omission when considering the transport and the fate of ACT in complex and dynamics systems, such as estuaries and coastal lagoons. Over the coming years, the concentration of chloride ions and DOM in estuaries and coastal lagoons are likely to experience high fluctuations due to global climate change (GCC) [26,27]. It has been projected that

* Corresponding author at: Chemistry Department, LAQV – REQUIMTE, FCT-UNL, Campus da Caparica, 2829-516, Caparica, Portugal.
E-mail address: jpnoronha@fct.unl.pt (J.P. Noronha).

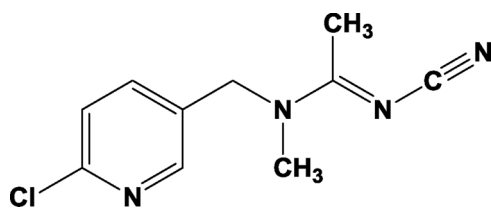


Fig. 1. Molecular structure of acetamiprid (IUPAC name: (*E*)-*N*1-[(6-chloro-3-pyridyl)methyl]-*N*2-cyano-*N*1-methylacetamidine).

about 70% of coastlines worldwide are likely to experience sea level change in the next decades due to GCC [27]. A rise of the sea level will affect the salinity of the lagoons through inundation [26]. Alterations of the rainfall patterns and an increase in extreme weather events (intense precipitation vs. drought) will have an impact on water salinity and consequently on chloride concentration [26]. Changes in the rainfall patterns are also likely to influence the amount and type of DOM present in estuaries and lagoons as well as the concentration of pollutants due to soil runoff [26,28]. Climate change can also alter the exposure of ecosystems to UV-B radiation by influencing the Earth system processes that affect ozone depletion [20,25,28–32]. UV radiation (280–400 nm), including UV-B and UV-A, modifies carbon cycling through changes in its capture and will potentially disturb DOM distribution and content [20,25,28–32]. GCC associated with interactions with solar UV radiation are likely to influence the environmental fate of pesticides. An understanding of the processes involved in the photodegradation of pesticides in fresh and saline waters will allow in a near future a better prediction of the behaviour of pesticides, especially in coastal lagoons under GCC. Studies of pesticide photodegradation are also important for the management of wastewater treatment plants that apply UV radiation in degradation/mineralization processes [33]. In view of this, the aim of this study was to investigate the photodegradation kinetics of ACT in fresh and saline waters and to evaluate the influence of pH, salinity and DOM on its photodegradation kinetics. Photodegradation experiments were carried out in model water matrices as well as in natural waters taken from a coastal lagoon after a period of heavy rain for a general overview of the effects of the predicted GCC on the environmental fate of ACT.

2. Materials and methods

2.1. Reagents

Acetonitrile (HPLC grade) was purchased from Carlo Erba (Val de Reuil, France). Formic acid (ACS reagent), anhydrous sodium sulphate p.a and sodium chloride p.a were bought from Panreac (Barcelona, Spain). Sodium iodide p.a and sodium bromide p.a were purchased from Sigma-Aldrich (St. Louis, MO, USA). Acetamiprid (99.9%, CAS 135410-20-7), Aldrich humic acid (AHA), isopropanol p.a and Whatman GF/F glass microfiber filters (0.7 µm nominal pore-size) were obtained from Sigma-Aldrich (St. Louis, MO, USA). Potassium dihydrogen phosphate p.a (KH₂PO₄) and di-potassium hydrogen phosphate anhydrous (K₂HPO₄) were obtained from Merck (Darmstadt, Germany). Suwannee River natural organic matter (SRNOM, 2R101N) and Suwannee River fulvic acid (SRFA, 2S101F) were purchased from the International Humic Substances Society (IHSS, St. Paul MN, USA). Water employed in all experiments was Milli-Q® grade.

2.2. Sampling

Water samples were collected in April 2016 in three sites (1, 2 and 3) (Óbidos Lagoon (OL)), a coastal lagoon located on the West coast of Portugal (Fig. 2). A sample was also collected at the confluence point of two rivers (Arnóia and Real River, site 4) that drain into the lagoon to evaluate the effect of freshwater on the photodegradation of ACT. After

collection, water samples were filtered through pre-combusted Whatman GF/F glass microfiber filters (0.7 µm nominal pore-size) and kept at 4 °C for photolysis experiments, which were made within 48 h of collection.

2.3. UV-vis and ATR-FTIR spectroscopy

The UV-vis absorption spectra of water samples were measured on a Spectronic Helios alpha dual-beam spectrophotometer (Thermo Scientific, Waltham, MA, USA) using 1 cm path length quartz cuvettes. To minimize temperature effects, samples were equilibrated at room temperature. Specific UV absorbance (SUVA_{254nm}, L mg-C⁻¹ m⁻¹) was calculated by normalization of the UV absorbance at λ 254 nm (m⁻¹) with the concentration of the dissolved organic carbon (DOC, mg-C L⁻¹) [34]. Attenuated Total Reflectance – Fourier Transform Infrared (ATR-FTIR) spectra were recorded with a PerkinElmer Spectrum Two FTIR spectrometer (PerkinElmer Inc., Waltham, MA, USA) equipped with a UATR two attenuated total reflectance (ATR) sampling accessory with a single reflection diamond crystal. The FTIR spectra were averaged from 4 scans and recorded over the range of 4500–450 cm⁻¹ at a resolution of 4 cm⁻¹.

2.4. Determination of acetamiprid by HPLC-DAD

High performance liquid chromatography (HPLC) analyses were carried out using a Waters® 2690 separation module (Milford, MA, USA) coupled to a photodiode array detector (DAD) (Waters™ 996) and equipped with a Phenomenex Kinetex 2.6 µm XB-C18 (150 × 4.6 mm i.d.) column and a Phenomenex security guard column (security guard™ cartridges, C18, 4 × 3 mm i.d.) (Torrence, CA, USA). Injection volume was 25 µL and compounds were eluted in isocratic mode with acetonitrile at 30% and MilliQ® water (0.1% formic acid) at 70%. The flow rate was set at 0.5 mL min⁻¹. The chromatograms were acquired with a MassLynx™ software data acquisition system. Acetamiprid was quantified at 245 nm using a calibration curve with 6 ACT standards solutions. Limit of quantification was 0.01 mg L⁻¹ and the precision measured in terms of relative standard deviation (RSD) was ≤15%.

2.5. Irradiation experiments

2.5.1. Photolysis – MP Hg lamp

Photodegradation studies were carried out in a 300 mL pear-shaped glass reactor (exterior) with a medium pressure mercury (MP Hg) lamp (150 W) inside that emits radiation in the range of 200 to 400 nm, as described elsewhere [33]. The lamp was cooled to 20 ± 2 °C with tap water using a quartz-cooling jacket. Samples were irradiated for 15 min under aerated conditions. 2 mL samples were taken at 0, 1, 2, 3, 5, 10, 15, 20 and 30 min, for acetamiprid analysis by HPLC-DAD. The ACT concentration used in the experiments was 5.0 mg L⁻¹ to easily understand the effect of the photolysis in the target compound and also to compare with data from other studies that use the same ACT concentration [10]. Photolysis experiments were carried out with ACT solution (5.0 mg L⁻¹) prepared in: (a) unbuffered MilliQ® water (0.80 µScm⁻¹) with and without the addition of AHA (5, 10, 15, 20 and 25 mg L⁻¹), SRNOM (10 and 20 mg L⁻¹) and SRFA (10 and 20 mg L⁻¹); (b) 10 mmol L⁻¹ phosphate buffer at pH 5, 7 and 9; (c) sodium chloride (NaCl) solutions 20 and 35 g L⁻¹; (d) NaCl solution (35 g L⁻¹) with AHA (10 mg L⁻¹) and isopropanol 20 mmol L⁻¹; (e) Na₂SO₄ 0.20 mol L⁻¹; (f) NaI and NaBr solutions 0.60 mol L⁻¹ and (g) saline and fresh water collected from a coastal lagoon (Óbidos Lagoon) and a tributary that drains into the lagoon, respectively (Fig. 2). Control samples (2 mL of ACT solution) were placed in the dark in closed vials and analysed by HPLC-DAD at the beginning of the photolysis and after 72 h. All experiments were run in triplicate.

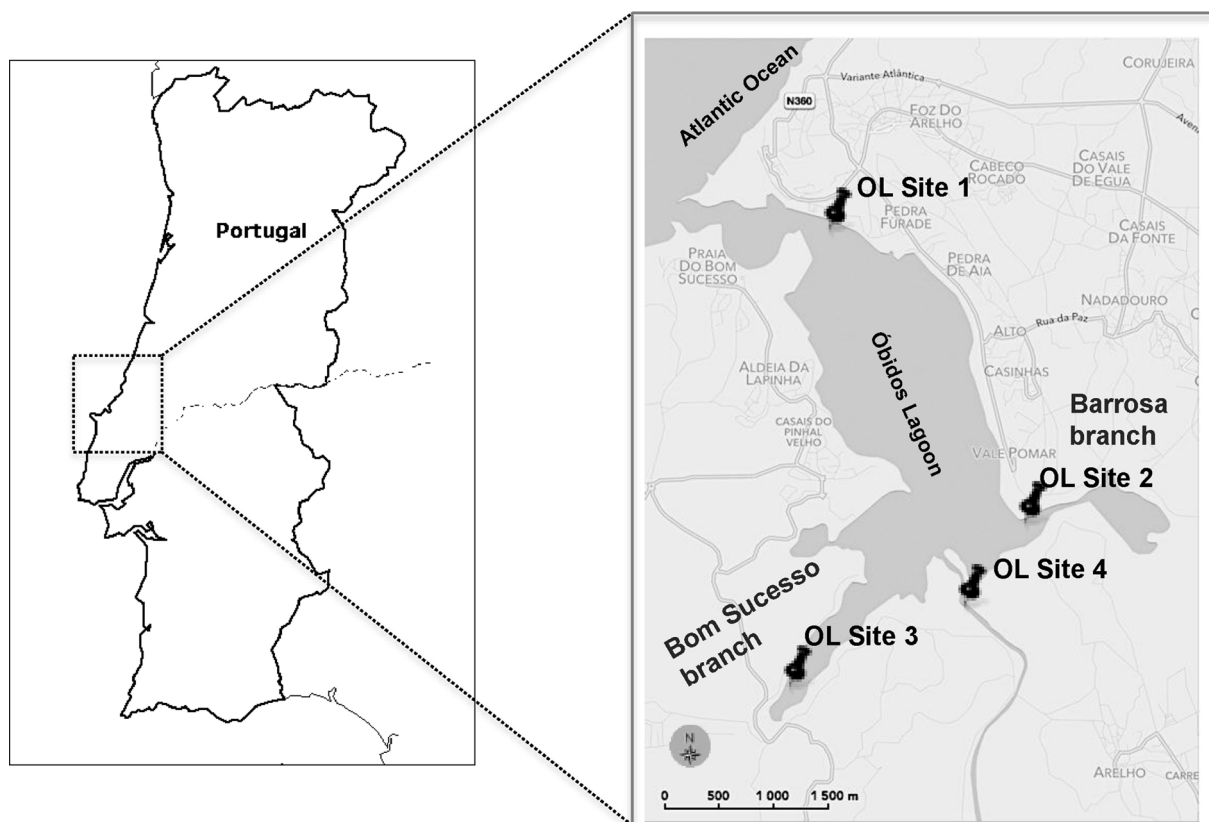


Fig. 2. Óbidos Lagoon (OL) – Water sampling sites: OL site 1 (near the lagoon inlet), OL site 2 (Barrosa branch), OL site 3 (Bom Sucesso branch) and OL site 4 (confluence of Real and Arnóia River before their discharge into the OL).

2.5.2. Photodegradation rate constants

The pseudo-first-order rate constants (k_p) for photodegradation of ACT in the aqueous solutions were calculated using Eq. (1):

$$\ln \left[\frac{C_t}{C_0} \right] = -k_p t \quad (1)$$

where, t is the irradiation time, C_t is the residual concentration of ACT at time t and C_0 its initial concentration. Half-life times ($t_{1/2}$) were calculated using Eq. (2):

$$t_{1/2} = \frac{0.693}{k_p} \quad (2)$$

Comparison of k_p mean values was done statistically by analysis of variances (ANOVA) [35]. Acceptance or rejection of the null hypothesis was based on an α -level of 0.05 [35].

3. Results and discussion

3.1. Photodegradation of ACT in model water matrices

Experiments were carried out with model water matrices at different pH's, salinities and different types/concentrations of DOM (AHA, SRNOM and SRFA) to evaluate their effect on the photodegradation of ACT, photodegradation. Sodium and chloride ions represent about 91% of all seawater ions, even though there are smaller quantities of other ions in seawaters (e.g., K^+ , Mg^{2+} , or SO_4^{2-}), and therefore the effect of salinity was based on the effect of chloride ions. In all experiments, photodegradation of ACT followed a pseudo-first-order kinetics with determination coefficients (r^2) ≥ 0.97 (Tables 1 and 2). The loss of ACT in control samples in the dark was $< 2\%$ of the initial concentration, and degradation was therefore attributed only to photolysis.

Table 1

Photodegradation rate constants (k_p) of acetamidrid (5.0 mg L^{-1}) dissolved in different aqueous matrices (different pH and salt concentration with and without isopropanol and AHA) under MP Hg lamp irradiation. k_p values are presented as mean value \pm standard deviation ($n = 3$). pK_a acetamidrid = 0.7 at 25°C [6,8].

Aqueous matrix	k_p (min^{-1})	r^{2a}	$t_{1/2}$ (min)	Salinity (g L^{-1})
Unbuffered MilliQ® water	0.56 ± 0.14	0.97	1.2	–
Buffered MilliQ® water ($10 \text{ mmol L}^{-1} \text{ PO}_4^{3-}$)				
pH 5.0	0.60 ± 0.01	0.98	1.2	–
pH 7.0	0.60 ± 0.05	0.97	1.2	–
pH 9.0	0.57 ± 0.05	0.99	1.2	–
Saline solutions				
NaCl 20 g L^{-1} (0.34 mol L^{-1})	0.74 ± 0.02	0.97	0.94	20
NaCl 35 g L^{-1} (0.60 mol L^{-1})	0.87 ± 0.08	0.97	0.79	35
NaBr 61.7 g L^{-1} (0.60 mol L^{-1})	0.68 ± 0.02	0.99	1.0	36
NaI 89.9 g L^{-1} (0.60 mol L^{-1})	0.11 ± 0.02	0.98	6.1	38
Na_2SO_4 28.4 g L^{-1} (0.20 mol L^{-1})	0.74 ± 0.02	0.97	0.94	22
NaCl 35 g L^{-1} + Isopropanol 1.20 g L^{-1} (20 mmol L^{-1})	0.73 ± 0.02	0.98	0.95	35
NaCl 35 g L^{-1} + AHA ^b 10 mg L^{-1}	0.57 ± 0.01	0.98	1.2	35

^a r^2 – Coefficient of determination.

^b AHA – Aldrich Humic Acid.

3.1.1. Effect of pH, salinity and dissolved organic matter (DOM)

The results show that an increase of pH from 5 to 9 did not have a significant impact on the photodegradation rate constants (k_p) of ACT, or the corresponding half-life times ($t_{1/2}$) (Table 1). However, the addition of sodium chloride to unbuffered MilliQ® water increased k_p significantly (Table 1), and the increase continued upon increasing NaCl concentration from 20 and 35 g L^{-1} . However, the degradation rate constants are not significantly different from each other (ANOVA,

Table 2

Photodegradation rate constants (k_p) of acetamidrid (5.0 mg L^{-1}) dissolved in aqueous matrices at different DOM type/concentrations (AHA, SRNOM and SRFA) under MP Hg lamp irradiation. k_p , and $\text{SUVA}_{254\text{nm}}$ values are presented as mean value \pm standard deviation ($n = 3$).

Aqueous matrix	k _p (min ⁻¹)	r ^{2a}	t _{1/2} (min)	DOC ^b (mg L ⁻¹)	SUVA _{254nm} ^c (L mg·C ⁻¹ m ⁻¹)
<i>Aldrich Humic Acid (AHA)</i>					
AHA 2.5 mg L ⁻¹	0.47 ± 0.08	0.98	1.5	2.3	5.9 ± 0.4
AHA 5.0 mg L ⁻¹	0.60 ± 0.01	0.98	1.2	3.9	
AHA 10 mg L ⁻¹	0.51 ± 0.05	0.98	1.4	7.1	
AHA 15 mg L ⁻¹	0.35 ± 0.02	0.97	2.0	10	
AHA 20 mg L ⁻¹	0.40 ± 0.01	0.99	1.8	14	
AHA 25 mg L ⁻¹	0.22 ± 0.01	0.99	3.1	17	
<i>Suwannee River Natural Organic Matter (SRNOM)</i>					
SRNOM 10 mg L ⁻¹	0.42 ± 0.02	0.98	1.6	5.1	4.1 ± 0.3
SRNOM 20 mg L ⁻¹	0.30 ± 0.02	0.98	2.3	10	
<i>Suwannee River Fulvic Acid (SRFA)</i>					
SRFA 10 mg L ⁻¹	0.31 ± 0.03	0.99	2.2	5.3	4.6 ± 0.3
SRFA 20 mg L ⁻¹	0.30 ± 0.02	0.99	2.3	11	

^a r^2 – Coefficient of determination.

^b DOC – Dissolved organic carbon.

^c SUVA – Specific UV absorbance determined at λ 254 nm (calculated by normalization of the UV absorbance at λ 254 nm (divided by cell path length, m^{-1}), with the concentration of the DOC).

$p < 0.05$). In contrast, bromide ions (Br^-) appear to have less catalytic effect than chloride ions (Table 1), while the effect of iodide ions (I^-) was even smaller. In general, halide ions (X^-) are very stable, however, under certain conditions they can produce the corresponding reactive halogen species (RHS; $\text{X}\cdot$, $\text{X}_2\cdot^-$) [36–40]. The radicals $\text{X}_2\cdot^-$ are less reactive than $\text{HO}\cdot$ while the $\text{X}\cdot$ radicals have been described as rival of $\text{HO}\cdot$ in the magnitude of their rate constants with organic compounds [36]. At the halide ion concentrations used, halogen atoms will react very rapidly with the anions to form the $\text{X}_2\cdot^-$ radical anions. Although speculation of possible mechanistic pathways in natural waters is complicated due to the many species present, it can provide useful insights into the photodegradation. We will concentrate on what are likely to be the dominant oxidizing species in saline waters, hydroxyl radicals and halogen atoms/dihalide radical anions ($\text{X}_2\cdot^-$). Possible routes to photochemical formation of hydroxyl radicals in natural waters have been discussed in detail elsewhere [41,42]. Both direct [43] and sensitized [44] photolysis can be used to produce halogen atoms in aqueous solutions; these react rapidly with excess of halide ion to produce the corresponding dihalide radical anions ($\text{X}_2\cdot^-$) as the dominant species. Normally the UV absorption of halide ions under environmentally relevant conditions is at too short wavelengths for the direct excitation process to be relevant [44], and photosensitization routes are dominant. However, since the halide absorption involves a charge-transfer-to-solvent transition, the band is strongly solvent dependent, and is shifted to longer wavelengths in the presence of organic materials [45], which may permit some halide ion photolysis. Halide ions are also oxidized by hydroxyl radicals, with initial reversible formation of the $\text{XOH}\cdot^-$ radical anion, which subsequently reacts with halide ions to produce $\text{X}_2\cdot^-$ [39,40]. Bromide ions are better scavengers of $\text{HO}\cdot$ radicals, with reaction rate constant ($1.1 \times 10^{10} \text{ Ms}^{-1}$) greater than that for chloride ($4.3 \times 10^9 \text{ Ms}^{-1}$) [23]. In both cases, this means that in saline waters dihalide radical anions, (or other reactive halogen species, RHS [24] compete favourably with hydroxyl radicals in the oxidation of substrates. Hydroxyl radicals and $\text{X}_2\cdot^-$ radical anions show rather different reactivity, with much lower selectivity seen for hydroxyl radicals, which tend to react by addition or hydrogen abstraction, whereas a wide range of reactivities are seen with $\text{X}_2\cdot^-$, which can take part in electron transfer, halogen atom transfer and hydrogen abstraction processes [46,47]. The decrease in photodegradation rate of ACT on going from chloride to bromide to iodide seen in Table 1 parallels the order of reactivities of the dihalide radical anions $\text{Cl}_2\cdot^- > \text{Br}_2\cdot^- > \text{I}_2\cdot^-$ [47], supporting the involvement of these species in the photodegradation. This reflects the differences in the standard electrode potentials ($\text{Cl}_2\cdot^-/2\text{Cl}^- + 2.126 \text{ V}$; $\text{Br}_2\cdot^-/2\text{Br}^- +$

1.63 V ; $\text{I}_2\cdot^-/2\text{I}^- + 1.03 \text{ V}$ [48]. With iodide ions, there may be an additional (auto)inhibiting effect due to formation of triiodide ions that are formed during the photolytic process [36]. These are important results and contrast with those found by Silva et al. [49] where a weak quenching of naphthyl acetamide was observed in the presence of bromide ions and no significant quenching with chloride ions. In that case, charge transfer from anion to naphthyl acetamide occurs, which follows the order $\text{I}^- > \text{Br}^- > \text{Cl}^-$.

Although these results suggest the involvement of reactive halogen species in the photodegradation of ACT, addition of isopropanol, an $\text{HO}\cdot$ scavenger [37], in the presence of sodium chloride at 35 g L^{-1} reduced the value of k_p (Table 1), which may suggest the involvement of the $\text{HO}\cdot$ radical as well. However, this is not unambiguous, as $\text{Cl}_2\cdot^-$ radical anions do react with isopropanol [46]. A further explanation for this observation is that isopropanol also absorbs at the UV range and could be shading ACT from direct photolysis. Isopropanol shows a maximum of absorbance at 264 nm (probably due to traces of aromatic compounds used in azeotropic distillation) and at wavelengths below 220 nm where the spectral irradiance of the MP Hg UV lamp is very low (Fig. S1 and S3). As shown in Fig. S3, and for the concentrations used in the present study, the absorbance values for isopropanol (20 mM) are much lower than the absorbance of ACT at 5 ppm which, is an indication that this shading effect is not significant.

An increase of the ACT degradation rate (k_p) in presence of chloride ions (Cl^-) is, therefore, an indication that radical chloride species, probably $\text{Cl}_2\cdot^-$, are formed and that they are more present in higher concentrations than $\text{HO}\cdot$ in the indirect photodegradation of ACT. These results support the importance of the reactive chloride species ($\text{Cl}\cdot$, $\text{Cl}_2\cdot^-$) in saline waters on the photodegradation of ACT. The results also show that although the substitution of NaCl by the inert salt sodium sulphate (Na_2SO_4) at the same ionic strength as solution of NaCl 35 g L^{-1} (0.60 mol L^{-1}) decreased the value of k_p (Table 1), the degradation of ACT was faster in Na_2SO_4 than in unbuffered MillQ water, which suggests that ionic strength may also play a role in the mechanism of ACT photodegradation. DOM was also seen to play a role in the photodegradation of ACT in saline waters. As presented in Table 1, k_p was reduced to approximately 34% of that in NaCl 35 g L^{-1} in the presence of AHA at 10 mg L^{-1} .

DOM inhibitor effect can be due to light absorption of the DOM possibly leading to its photobleaching, or, by scavenging of reactive species (such as $\text{HO}\cdot$), and/or by limiting of the net oxidation due to reduction of ACT intermediates [20,22]. Goldstone et al. [50] observed that bleaching of humic substances by $\text{HO}\cdot$ reaction was relatively slow except in waters with very high $\text{HO}\cdot$ photo transformation rates. Hence,

under the conditions used in this study, $\text{HO}\cdot$ scavenging by DOM might not be the main reason for a decrease of $\text{ACT } k_p$. DOM photobleaching is a plausible hypothesis for $\text{ACT } k_p$ decay and is inline with our previous work [51]. Photobleaching destroys the chromophores necessary for $^3\text{DOM}^*$ (excited triplet state of dissolved organic matter) formation, which leads to a loss of sensitized photolysis pathways [23]. For low concentrations of SRNOM (5 mg L^{-1}) photobleaching was suggested to be the dominant process of SRNOM transformation in the presence of high concentration of chloride (35 g L^{-1}) and chlorpyrifos at 1 mg L^{-1} [51]. The results are also in accordance with the findings of Grebel et al. [24,36]. The authors found out that the presence of Cl^- and Br^- ions at seawater concentrations enhanced absorbance photobleaching reactions rates by almost 40% regardless of the CDOM source [24]. It is possible, as suggested by Grebel et al. [36], that halide scavenging of $\text{HO}\cdot$ will form reactive halogen radicals that target electron-rich chromophores within DOM more selectively than $\text{HO}\cdot$. This may be a consequence of inherent differences in reactivity and the longer lifetimes of the halogen radicals, such as $\text{Cl}_2^{\cdot-}$, in water. A decrease of the $\text{ACT } k_p$ in the presence of AHA is therefore a strong indication of the formation of the radical chloride species ($\text{Cl}\cdot$, $\text{Cl}_2^{\cdot-}$) in saline waters and their possible scavenger by the more electron-rich chromophores present in AHA. Other compounds like 17β -estradiol have also shown a decrease of their degradation rate in saline water compared to fresh waters in the presence of DOM [52]. Increasing halide concentrations up to seawater levels decreased the photolysis rate of 17β -estradiol by 90%, with approximately 70% of this decrease associated with ionic strength effects, and the remainder 30% due to halide-specific effects. Halide promotion of NOM chromophore photobleaching was shown to play a major role in the halide-specific effect [52]. A decrease of the photodegradation rate of ACT in saline waters in the presence of DOM can also be a consequence of an increase of the ionic strength which inhibits the electron transfers pathways, lengthening the triplet lifetimes and promoting triplet–triplet reactions [53].

3.1.2. Inhibitor effect of DOM

To evaluate the inhibitor effect of DOM on the photodegradation rate of ACT in systems in the absence of chloride, experiments were carried out at different concentrations of AHA, SRNOM and SRFA (Table 2). As can be seen from Fig. 3, k_p showed a tendency to decrease in the presence of high concentrations of AHA. In SRNOM and SRFA (Table 2), k_p was significantly lower than that in MilliQ water (Table 1). In contrast to the behaviour with AHA and SRNOM, an increase of SFRA from 10 mg L^{-1} (5.1 mg L^{-1} DOC) to 20 mg L^{-1} (10 mg L^{-1} DOC) did not have any significant impact on the values of k_p and related $t_{1/2}$ (ANOVA, $p < 0.05$).

The influence of AHA, SRNOM and SFRA on the photodegradation

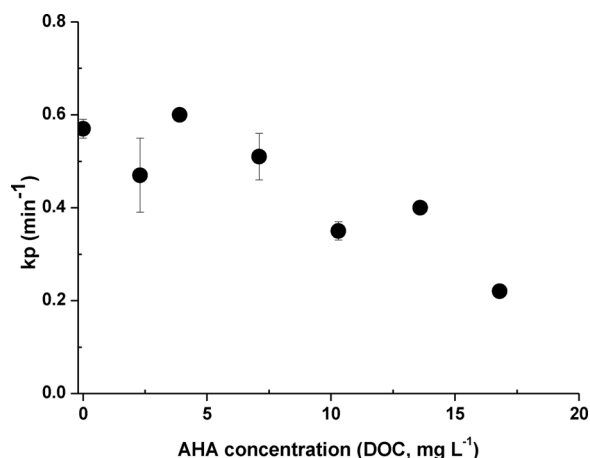


Fig. 3. Photodegradation rate constants of acetamiprid (5.0 mg L^{-1}) as a function of AHA concentration expressed in terms of DOC (mg L^{-1}).

of ACT is likely related to their complex chemical structure. $\text{SUVA}_{254\text{nm}}$ is a parameter that has been used as a surrogate measurement for DOM aromaticity and molecular weight (MW) [16,34,54]. High values of $\text{SUVA}_{254\text{nm}}$ are an indication of DOM with a high aromatic content and high MW fractions [20,54–56]. As shown in Table 2, AHA was found to have the highest value of $\text{SUVA}_{254\text{nm}}$. This is an indication that AHA is likely to have a relatively higher content of hydrophobic, aromatic and high MW material than SRNOM and/or SRFA. AHA is derived from brown coal while SRNOM and SRFA are obtained from natural aquatic organic matter [16]. Although complex, the FTIR spectra of SRNOM, AHA and SRFA show some differences especially for SRFA that shows two intense bands at 1658 and 1115 cm^{-1} (Fig. S4). The band at 1658 cm^{-1} can be due to the overlap of the aromatic $\text{C}=\text{C}$ stretching bands conjugated with $\text{C}=\text{O}$ and/or COO^- stretching ones, together with, keto $\text{C}=\text{O}$ and the $\text{N}-\text{H}$ bending of amides [57–61]. The intense band of SRFA at 1115 cm^{-1} has been assigned to the vibrations of the alcoholic hydroxyl group, phenols and carbohydrates/polysaccharides and can be an indication that SRFA is likely to have more oxygen functional groups than the other two DOM standards [61–64]. The results presented herein are in agreement with the findings of Batista et al. [16]. In addition to the increase of $\text{SUVA}_{254\text{nm}}$ from SRFA (\approx SRNOM) to AHA, Batista et al. [16] also found out by the analysis of ^1H NMR spectra that the percentage of aromatic content was greater for AHA (37%) than for SRFA (22%) and SRNOM (21%) [16]. In their work, SRFA and SRNOM showed a higher percentage (in the range of 33–36%) of carboxylic-rich alicyclic molecules (CRAM) and of carbohydrates/proteins (18–21%) [16]. The higher content of CRAM and carbohydrate/proteins in the SRFA and SRNOM standards might explain the broad peak at 1658 cm^{-1} found in the FTIR spectra (Fig. S4).

Due to its complex chemical structure DOM has been implicated as both a sensitizer and an inhibitor of the photodegradation of pesticides, polycyclic aromatic hydrocarbons and some antibiotics [10,14,20,21,50,65,66]. The exposure of DOM to UV–vis radiation generates a variety of reactive species, known as photochemically produced intermediates (PPRIs), in particular, singlet oxygen ($^1\text{O}_2$), superoxide ($\text{O}_2^{\cdot-}$) and its dismutation product hydrogen peroxide (H_2O_2), aqueous electron ($\text{e}^-(\text{aq.})$), hydroxyl radical ($\text{HO}\cdot$) and excited triplet states of DOM ($^3\text{DOM}^*$) [20]. Vaughan et al., 1998 shows that SRFA exhibits a dioxygen-independent pathway of $\text{HO}\cdot$ production and it cannot be due only to anions photolysis (e.g. nitrite or nitrate) [41]. $\text{HO}\cdot$ can be generated directly by the photolysis of DOM, excited triplet state of benzoquinone and certain substituted benzoquinones is capable of abstracting a hydrogen atom from water to generate $\text{HO}\cdot$ [41]. Dell’Arcipetre et al. [11,12,67] studied the chemical reaction of ACT with $^1\text{O}_2$, $\text{HO}\cdot$, and $^3\text{DOM}^*$ (using Rose Bengal triplet state as sensitizer) and obtained reaction rate constants of the order of $1.3 \pm 1 \times 10^6$, $5.5 \pm 1 \times 10^{10}$ and $3.6 \pm 1 \times 10^7 \text{ Ms}^{-1}$, respectively. Although the reaction of ACT with $\text{HO}\cdot$ seems to be more fast/favorable, the results reported herein show that the DOM standards, AHA, SRNOM and SRFA have an inhibiting effect on the photodegradation rate of ACT. The slowdown of k_p is probably due to DOM photobleaching as well as its antioxidant properties. Several studies have shown that in aerated conditions DOM is capable of inhibit the triplet-induced transformation oxidation intermediates of various organic compounds especially aromatic nitrogen compounds [17,21,22]. In aerated conditions $^3\text{DOM}^*$ is the precursor of $^1\text{O}_2$ [23]. Both reactive species can react with ACT in agreement with the reported mechanisms for the reactions of $^1\text{O}_2$ and Rose Bengal triplet state ($^3\text{RB}^*$) with ACT [11]. The mechanism presented in scheme of Fig. 4 was also based in the conceptual model for the triplet-induced oxidation of a contaminant and subsequent inhibition reported by Wenk et al. [21]. As shown in Fig. 4, it is possible that the ACT radical formed by reaction with $^1\text{O}_2$ or $^3\text{DOM}^*$ will be reduced back to ACT by the electron donor capacities of several moieties that might be present in DOM, such as phenols, polyhydroxylated aromatics, indoles, etc. The lower value of the photodegradation rate constant of ACT in the presence of SRFA can therefore

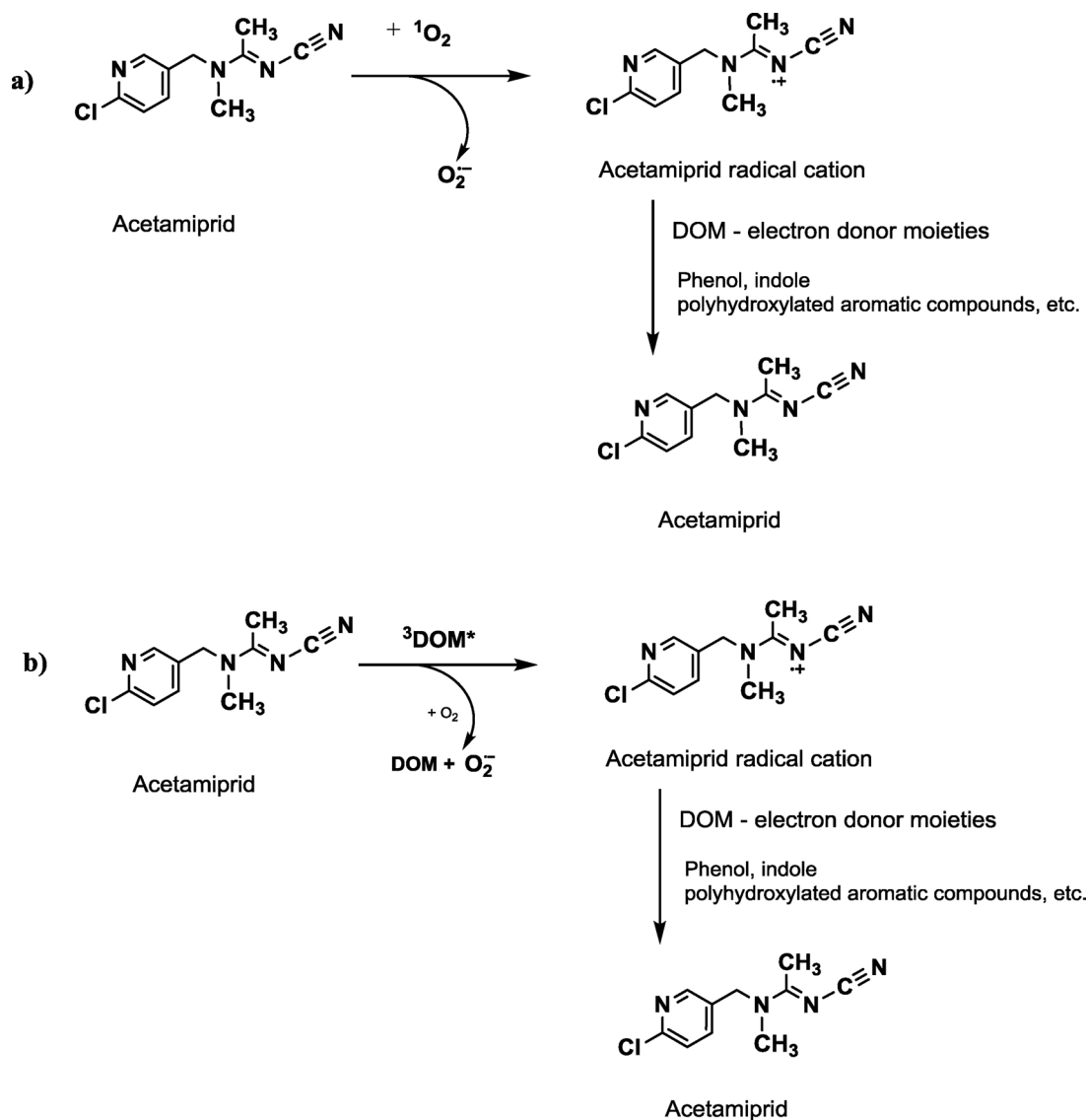


Fig. 4. Scheme of a potential mechanism of acetamiprid radical inhibition by dissolved organic matter (DOM) due to the presence electron donor groups/moieties like phenols, polyhydroxylated aromatic, indole, etc. **a)** Acetamiprid radical induced by singlet oxygen ($^1\text{O}_2$); **b)** Acetamiprid radical induced by excited triplet states of DOM ($^3\text{DOM}^*$).

be a consequence of high contents of such type of functional groups as suggested by its respective FTIR spectrum (Fig. S4). AHA is more aromatic and, therefore, its inhibiting effect is greater for higher concentrations. ACT is only slightly degraded by direct photolysis under solar radiation, mainly because its absorption maximum is in the UV range at 216 and 245 nm; nevertheless the formation of $^3\text{DOM}^*$ and $^1\text{O}_2$ in aquatic systems due to the presence of DOM will have an impact on its degradation/persistence and its environmental fate.

3.2. Photodegradation of ACT in natural waters and its environmental relevance

Several experiments were carried out to evaluate the photodegradation of ACT in natural waters using samples taken from Óbidos Lagoon (OL, Fig. 2). As shown in Fig. 5, photodegradation of ACT in natural waters followed a pseudo-first-order kinetics with photodegradation rate constants (k_p) between 0.50–0.72 min^{-1} and half-life times ($t_{1/2}$) in the range of 0.90–2.0 min (Table 3).

Results show that k_p increased in the following order: OL site 4 < OL site 2 < OL site 1 < OL site 3 (Table 3). The k_p of OL site 2 is higher than that of OL site 4 probably as a consequence of an increase of

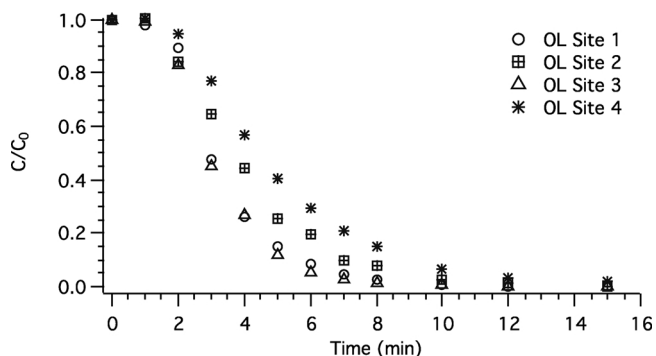


Fig. 5. Photochemical degradation of acetamiprid dissolved (5.0 mg L^{-1}) in water samples collected from Óbidos Lagoon (OL) as a function of the UV irradiation time.

water salinity and a decrease of DOC of OL site 2 (Table 3). The others two sites, OL site 1 and OL site 3, with higher salinities and lower content of organic matter associated with higher k_p values. No statistical difference was found between k_p of OL site 1 and OL site 3

Table 3

Photodegradation rate constants (k_p) of acetamiprid (5.0 mg L^{-1}) dissolved in natural waters collected from Óbidos Lagoon (OL) and some of its physico-chemical properties (pH, salinity and DOC). k_p values are presented as mean value \pm standard deviation ($n = 3$).

Water	OL location	k_p (min^{-1})	$t_{(1/2)}$ (min)	pH	Salinity (g L^{-1})	DOC ^a (mg C L^{-1})	SUVA _{254nm} ^b ($\text{L mg}^{-1} \text{ m}^{-1}$)
OL site1	Inlet	0.63 ± 0.12	1.1	8.34	32	< 2	< 0.30
OL site 2	Barrosa branch	0.50 ± 0.03	1.4	8.07	15	5.4	2.4
OL site 3	Bom Sucesso branch	0.72 ± 0.03	0.9	8.17	34	< 2	< 1.4
OL site 4	Confluence of two rivers	0.35 ± 0.05	2.0	7.53	0.3	9.0	2.5

^a DOC – Dissolved organic carbon.

^b SUVA – Specific UV absorbance determined at 254 nm.

(ANOVA, $p < 0.05$). No relation was found between k_p of ACT and the pH (Table 3).

Table 3 shows that k_p has a tendency to increase with an increase of salinity and to decrease in the presence of DOM. This is inline with the findings obtained for the model water model matrices studied (Tables 1 and 2). As shown in Table 3, the water samples collected inside the lagoon (OL site 1, OL site 2 and OL site 3) showed a variation in salinity, pH and DOM concentration/characteristics, especially at OL site 2. The reason for such variations in the salinity and other parameters, especially at OL site 2, was that water samples were collected after a period of heavy rain. The OL site 2 is located on the Barrosa branch (Fig. 2), which is a shallow area (0.5–1 m), such that it is more influenced by the freshwater inputs coming from the rain and the small tributaries that enter into the lagoon [68,69]. The identical value of SUVA_{254nm} (Table 3) of OL site 2 to OL site 4 and a decrease of its salinity is an indication of the input of terrestrial DOM/freshwaters. These physical-chemical variations due to a weather changes are likely to be highly relevant to the photodegradation/persistence of ACT. In the case of contamination due to soil runoff or other source, ACT distribution/concentration along the lagoon is likely to be affected and its persistence will be more pronounced in case of high inputs of fresh and rain waters. In this way, variations found along OL can work as an initial alert/overview of the impact of predicted global climate change on the environmental fate of acetamiprid.

4. Conclusions

The results presented indicate the importance of the salinity and the concentration and characteristics/properties of the dissolved organic matter (DOM) on the photodegradation kinetics of acetamiprid (ACT) in water. The corresponding photodegradation rate constants, k_p , show a tendency to increase with an increase of salinity/chloride ions and to decrease in the presence of DOM. The formation of selective chloride radical species (Cl^- , $\text{Cl}_2^{\cdot -}$), DOM photobleaching, in addition to DOM inhibition/antioxidant properties are important parameters that should be taken into account in studies concerning the environmental fate of ACT in coastal waters. Due to global climate change, coastal lagoons are likely to experience in the coming decades high salinity and DOM fluctuations. Such variations will be reflected in the degradation/persistence and distribution of ACT especially within small coastal lagoons that will be highly influenced by GCC.

Acknowledgments

This work was supported by the Associate Laboratory for Green Chemistry LAQV which is financed by national funds from FCT/MEC (UID/UI/50006/2013) and co-financed by the ERDF under the PT2020 Partnership Agreement (POCI-01-0145-FEDER – 007265). The authors acknowledge the Instituto Politécnico de Setúbal (IPS) through the project 3CP-IPS-7-2009. HDB thanks CQC for support through the projects UID/UI/0313/2013 (FCT) and COMPETE.

Appendix A. Supplementary data

Supplementary data associated with this article can be found, in the online version, at <https://doi.org/10.1016/j.jphotochem.2018.04.020>.

References

- [1] European Commission (EC), Sanco/1392/2001 – Final, (2004) (16 June 2004: Acetamiprid).
- [2] E.E. Mitsika, C. Christophoros, K. Flytianos, Fenton and Fenton-like oxidation of pesticide acetamiprid in water samples: kinetic study of the degradation and optimisation using response surface methodology, *Chemosphere* 93 (2013) 1818–1825.
- [3] C. Bass, I. Denholm, M.S. Williamson, R. Nauen, The global status of insect to neonicotinoid insecticides, *Pest. Biochem. Physiol.* 121 (2015) 78–87.
- [4] N. Simon-Delso, V. Amaral-Rogers, L.P. Belzunces, J.M. Bonmatin, M. Chagnon, C. Downs, L. Furlan, D.W. Gibbons, C. Giorio, D. Girolami, D.P. Kreuzweiser, C.H. Krupke, M. Liess, E.M.M. Long, P. Mineau, E.A.D. Mitchell, C.A. Morrissey, D.A. Noome, L. Pisa, J. Settele, J.D. Stark, A. Tapparo, H.V. Dyck, J.V. Praagh, J.P. Sluijs, R.P. Whitehorn, M. Wiemers, Systemic insecticides (neonicotinoids and fipronil): trends, uses, mode of action and metabolites, *Environ. Sci. Pollut. Res.* 22 (2015) 5–34.
- [5] J.P. Sluijs, N. Simon-Delso, D. Goulson, L. Maxim, J.-M. Bonmatin, L.P. Belzunces, Neonicotinoids: bee disorders and the sustainability of pollinator services, *Curr. Opin. Environ. Sustain.* 5 (2013) 293–305.
- [6] M.O. Barbosa, N.F.F. Moreira, A.R. Ribeiro, M.F.R. Pereira, A.M.T. Silva, Occurrence and removal of organic micro pollutants: an overview of the watch list of EU Decision 2015/495, *Water Res.* 94 (2016) 257–279.
- [7] V. Christen, F. Mittner, K. Fent, Molecular effects of neonicotinoids in honey bees (*Apis mellifera*), *Environ. Sci. Technol.* 50 (2016) 4071–4080.
- [8] F. Sánchez-Bayo, R.V. Hyne, Detection and analysis of neonicotinoids in river waters – development of a passive sampler for three commonly used insecticides, *Chemosphere* 99 (2014) 143–151.
- [9] European Union (EU). Decision 2015/495 of 20 March 2015 establishing a watch list of substances for Union-wide monitoring in the field of water policy pursuant to Directive 2008/105/EC of the European Parliament and of the Council. *Official J. Eur. Union* (24.03.2015) L 78/40, 2015.
- [10] L. Carlos, D.O. Mártire, M.C. Gonzalez, J. Gomis, A. Bernabeu, A.M. Amat, A. Arques, Photochemical fate of a mixture of emerging pollutants in the presence of humid substances, *Water Res.* 46 (2012) 4732–4740.
- [11] M.L. Dell'Arciprete, L. Santos-Juanes, A. Arques, R.F. Vercher, A.M. Amat, J.P. Furlong, D.O. Mártire, M.C. Gonzalez, Reactivity of neonicotinoid pesticides with singlet oxygen, *Catal. Today* 151 (2010) 137–142.
- [12] M.L. Dell'Arciprete, J.M. Soler, L. Santos-Juanes, A. Arques, D.O. Mártire, J.P. Furlong, M.C. Gonzalez, Reactivity of neonicotinoid insecticides with carbonate radicals, *Water Res.* 46 (2012) 3479–3489.
- [13] H.D. Burrows, L.M. Canle, J.A. Santaballa, S. Steenken, Reaction pathways and mechanisms of photodegradation of pesticides, *J. Photochem. Photobiol. B* 67 (June (2)) (2002) 71–108.
- [14] A. Khan, M.M. Haque, N.A. Mir, M. Muneer, C. Boxall, Heterogeneous photo catalysed degradation of an insecticide derivative acetamiprid in aqueous suspensions of semiconductor, *Desalination* 261 (2010) 169–174.
- [15] C. Sirtori, A. Aguera, I. Carra, Application of liquid chromatography quadrupole time-of-flight mass spectrometry to the identification of acetamiprid transformation products generated under oxidative processes in different water matrices, *Anal. Bioanal. Chem.* 406 (2014) 2549–2558.
- [16] A.P.S. Batista, A.C.S.C. Teixeira, W.J. Cooper, B.A. Cottrell, Correlating the chemical and spectroscopic characteristics of natural organic matter with the photodegradation of sulfamerazine, *Water Res.* 93 (2016) 20–29.
- [17] S. Canonica, H.U. Lauscher, Inhibitor effect of dissolved organic matter on triplet-induced oxidation of aquatic contaminants, *Photochem. Photobiol.* 7 (2008) 547–551.
- [18] B.A. Cottrell, S. Timko, L. Devera, A.K. Robinson, M. Gonsior, A.E. Vizenor, A.J. Simpson, W.J. Cooper, Photochemistry of excited-state species in natural waters: a role for particulate organic matter, *Water Res.* 47 (2013) 5189–5199.
- [19] C. Richard, S. Canonica, Aquatic photo transformation of organic contaminants induced by coloured dissolved natural organic matter, *Handb. Env. Chem.* 2 (2005) 299–323 (Part M).

- [20] C.M. Sharpless, N.V. Blough, The importance of charge-transfer interactions in determining chromophoric dissolved organic matter (CDOM) optical and photochemical properties, *Environ. Sci. Process Impacts* 16 (2014) 654–671.
- [21] J. Wenk, S. Canonica, Phenolic antioxidants inhibit the triplet-induced transformation of anilines and sulfonamide antibiotics in aqueous solution, *Environ. Sci. Technol.* 46 (2012) 5455–5462.
- [22] J. Wenk, U.V. Gunten, S. Canonica, Effect of dissolved organic matter on the transformation of contaminants induced by excited triplet states and the hydroxyl radical, *Environ. Sci. Technol.* 45 (2011) 1334–1340.
- [23] C.M. Glover, F.L. Rosario-Ortiz, Impact of halides on the photodegradation of reactive intermediates from organic matter, *Environ. Sci. Technol.* 47 (2013) 1349–1356.
- [24] J.E. Grebel, J.J. Pignatello, W. Song, W.J. Cooper, W.A. Mitch, Impact of halides on photobleaching of dissolved organic matter, *Mar. Chem.* 115 (2009) 134–144.
- [25] S.A. Timko, C. Romera-Castillo, R. Jaffe, W.J. Cooper, Photo-reactivity of natural dissolved organic matter from fresh to marine waters in the Florida Everglades, USA, *Environ. Sci. Impacts* 16 (2014) 866–878.
- [26] A. Anthony, J. Atwood, P. August, C. Byron, S. Cobb, C. Foster, C. Fry, A. Gold, K. Hagos, L. Heffner, D.Q. Kellogg, K. Lellis-Dibble, J.J. Opaluch, C. Oviatt, A. Pfeiffer-Herbert, N. Rohr, L. Smith, T. Smythe, J. Swiff, N. Vinthateiro, Coastal lagoons and climate change: ecological and social ramifications in U.S. Atlantic and Gulf Coast ecosystems, *Ecol. Soc.* 14 (2009).
- [27] IPCC, Summary for policymakers, in: T.F. Stocker, D. Qin, G.K. Plattner, M. Tignor, S.K. Allen, J. Boschung, A. Nauels, Y. Xia, V. Bex, P.M. Midgley (Eds.), *Climate Change 2013: The Physical Science Basis. Contribution of Working Group I to the Fifth Assessment Report of the Intergovernmental Panel on Climate Change*, Cambridge University Press, Cambridge, United Kingdom and New York, NY, USA, 2013, p. 2013.
- [28] D.J. Erickson, B. Sulzberger, R.G. Zepp, A.T. Austin, Effects of stratospheric ozone depletion solar UV radiation, and climate change on biogeochemical cycling: interactions and feedbacks, *Photochem. Photobiol. Sci.* 14 (2015) 127–148.
- [29] A.F. Bais, R.L. McKenzie, G. Bernhard, P.J. Aucamp, M. Ilyas, S. Madronich, K. Tourpali, Ozone depletion and climate change: impacts on UV radiation, *Photochem. Photobiol. Sci.* 14 (2015) 19–52.
- [30] T. Brinkmann, D. Sartorius, Photobleaching of humid rich dissolved organic matter, *Aquat. Sci.* 65 (2003) 415–424.
- [31] J.R. Helms, A. Stubbins, E.M. Perdue, N.W. Green, H. Chen, K. Mopper, Photochemical bleaching of oceanic dissolved organic matter and its effect on absorption spectral slope and fluorescence, *Mar. Chem.* 155 (2013) 81–91.
- [32] United Nations Environment Programme (UNEP), Environmental Effects of Ozone Depletion and Its Interaction with Climate Change: 2010 Assessment. The Environmental Effects Assessment Panel Report for 2010, (2010).
- [33] R. Salgado, V.J. Pereira, G. Carvalho, R. Soeiro, V. Gaffney, C. Almeida, V. Vale Cardoso, E. Ferreira, M.J. Benoliel, T.A. Ternes, A. Oehmen, M.A.M. Reis, J.P. Noronha, Photodegradation kinetics and transformation products of keto-profen, diclofenac and atenolol in pure water and treated wastewater, *J. Hazard. Mater.* 244–245 (2013) 516–527.
- [34] A.M. Hansen, T.E.C. Kraus, B.A. Pellerin, J.A. Fleck, B.D. Downing, B.A. Bergamaschi, Optical properties of dissolved organic matter (DOM): Effects of biological and photolytic degradation, *Limnol. Oceanogr.* 61 (2016) 1015–1032.
- [35] J.N. Miller, J.C. Miller, *Statistics and Chemometrics for Analytical Chemistry*, 5th ed., Harlow, England, 2005.
- [36] J.E. Grebel, J.J. Pignatello, W. Mitch, Effect of halide ions and carbonates on the organic contaminant degradation by hydroxyl radical-based advanced oxidation processes in saline waters, *Environ. Sci. Technol.* 44 (2010) 6822–6828.
- [37] Y.L. Qiao, Y. Zhang, C. Zhou, H. Xie, J. Chen, Effects of halide on photodegradation of sulfonamide antibiotics: formation of halogenated intermediates, *Water Res.* 102 (2016) 405–412.
- [38] J. Kalmár, É. Dóka, G. Lente, I. Fábian, Aqueous photochemical reactions of chloride, bromide, and iodide ions in a diode-array spectrophotometer. Autoinhibition in the photolysis of iodide ions, *Dalton Trans.* 43 (2014) 4862–4870.
- [39] G.G. Jayson, B.J. Parsons, A.J. Swallow, Some simple, highly reactive, inorganic chlorine derivatives in aqueous solution. Their formation using pulses of radiation and their role in the mechanism of the Fricke dosimeter, *J. Chem. Soc. Faraday Trans. 1* (69) (1973) 1597–1607.
- [40] D. Vione, V. Maurino, C. Minero, P. Calza, E. Pelizzetti, Phenol chlorination and photochlorination in the presence of chloride ions in homogeneous aqueous solution, *Environ. Sci. Technol.* 39 (2005) 5066–5075.
- [41] P.P. Vaughan, N.V. Blough, Photochemical formation of hydroxyl radical by constituents of natural waters, *Environ. Sci. Technol.* 32 (1998) 2947–2953.
- [42] D. Vione, G. Falletti, V. Maurino, C. Minero, E. Pelezzetti, M. Malandrino, R. Aiassa, R.-J. Olariu, C. Arsene, Sources and sinks of hydroxyl radicals upon irradiation of natural water samples, *Environ. Sci. Technol.* 40 (2006) 3775–3781.
- [43] J. Jortner, M. Ottolenghi, G. Stein, On photochemistry of aqueous solutions of chloride bromide and iodide ions, *J. Phys. Chem.* 68 (1964) 247–255.
- [44] Y. Yang, J.J. Pignatello, Participation of the halogens in photochemical reactions in natural and treated waters, *Molecules* 22 (2017) 1684.
- [45] M.J. Blandamer, T.R. Griffiths, L. Shields, M.C.R. Symons, Solvation spectra. Part 8. Ultra-violet absorption spectra of bromide and chloride ions in various solvents, *Trans. Faraday Soc.* 60 (1964) 1524–1531.
- [46] K. Hasegawa, P. Neta, Rate constants and mechanisms of reactions of $\text{Cl}_2^- \cdot$ radicals, *J. Phys. Chem.* 82 (1978) 854–857.
- [47] P. Neta, R.E. Huie, A.B. Ross, Rate constants for reactions of inorganic radicals in aqueous solution, *J. Phys. Chem. Ref. Data* 17 (1988) 1027–1284.
- [48] D.A. Armstrong, R.E. Huie, W.H. Koppenol, S.V. Lymar, G. Merényi, P. Neta, B. Ruscic, D.M. Stanbury, S. Steenkan, P. Wardman, Standard electrode potentials involving radicals in aqueous solution: inorganic radicals (IUPAC Technical Report), *Pure Appl. Chem.* 87 (2015) 1139–1150.
- [49] E.S. Silva, P. Wong-Wah-Chung, M. Sarakha, H.D. Burrows, Photophysical characterization of the plant growth regulator 2-(1-naphthyl) acetamide, *J. Photochem. Photobiol. A Chem.* 265 (2013) 29–40.
- [50] J.V. Goldstone, M.J. Pullin, S. Bertilsson, B.M. Voelker, Reactions of hydroxyl radical with humid substances Bleaching, mineralization, and production of bioavailable carbon substrates, *Environ. Sci. Technol.* 36 (2002) 364–372.
- [51] M.I. Pinto, R. Salgado, B.A. Cottrell, W.J. Cooper, H.D. Burrows, C. Vale, G. Sontag, J.P. Noronha, Influence of dissolved organic matter on the photodegradation and volatilisation kinetics of chlorpyrifos in coastal waters, *J. Photochem. Photobiol. A Chem.* 310 (2015) 189–196.
- [52] J.E. Grebel, J.J. Pignatello, W.A. Mitch, Impact of halide ions on natural organic matter-sensitized photolysis of 17 β -Estradiol in saline waters, *Environ. Sci. Technol.* 46 (2012) 7128–7134.
- [53] K.M. Parker, J.J. Pignatello, W.A. Mitch, Influence of ionic strength on triplet-state natural organic matter loss by energy transfer and electron transfer pathways, *Environ. Sci. Technol.* 47 (2013) 10987–10994.
- [54] S. Canonica, L. Meunier, U.V. Gunten, Phototransformation of selected pharmaceuticals during UV treatment of drinking water, *Water Res.* 42 (2008) 121–128.
- [55] J.L. Weishaar, G.R. Aiken, B.A. Bergamaschi, M.S. Fram, R. Fujii, K. Mopper, Evaluation of specific ultraviolet absorbance as an indicator of the chemical composition and reactivity of dissolved organic carbon, *Environ. Sci. Technol.* 37 (2003) 4702–4708.
- [56] J. Wenk, M. Aeschbacher, E. Salhi, S. Canonica, U.V. Gunten, M. Sander, Chemical oxidation of dissolved organic matter by chloride dioxide chloride, and ozone: effects on its optical and antioxidant properties, *Environ. Sci. Technol.* 47 (2013) 11147–11156.
- [57] R.R.E. Artz, S.J. Chapman, A.H.J. Robertson, J.M. Potts, F. Laggoun-Defarge, S. Gogo, L. Comont, J.R. Disnar, A.J. Francez, FTIR spectroscopy can be used as a screening tool for organic matter quality in regenerating cutover peatlands, *Soil Biol. Biochem.* 40 (2008) 515–527.
- [58] M. Fuentes, R. Baigorri, G. González-Gaitano, J. Garcia-Mina, The complementary use of 1H NMR, 13C NMR: FTIR and size exclusion chromatography to investigate the principal structural changes associated with composting of organic materials with diverse origin, *Org. Geochem.* 38 (2007) 2012–2023.
- [59] P.V.X. Hung, B.S. Oh, B.X. Tung, S.G. Oh, K.S. Kim, S.J. Kim, S.H. Moon, I.S. Kim, A. Jang, Reflection of the structural distinctions of source – different humid substances on organic fouling behaviors of SWRO membranes, *Desalination* 318 (2013) 72–78.
- [60] J.I. Kim, G. Buckau, R. Klenze, D.S. Rhee, H. Wimmer, Nuclear Science and Technology: Characterization and Complexation of Humid Acids – Final Report, Commission of the European Communities, Luxembourg, 1991.
- [61] C. Landry, L. Tremblay, Compositional differences between size and classes of dissolved organic matter from freshwater and seawater revealed by an HPLC-FTIR system, *Environ. Sci. Technol.* 46 (2012) 1700–1707.
- [62] H.A.N. Abdulla, E.C. Minor, R.F. Dias, P.G. Hatcher, Changes in the compound classes of dissolvers organic matter along estuarine transect: a study using FTIR and ^{13}C NMR, *Geochim. Cosmochim. Acta* 74 (2010) 3815–3838.
- [63] J. Coates, Interpretation of infrared spectra: a practical approach, in: R.A. Meyers (Ed.), *Encyclopedia of Analytical Chemistry*, John Wiley & Sons Ltd., Chichester, 2000, pp. 10815–10837.
- [64] M. Mecozzi, E. Pietrantonio, M. Pietroletti, The role of carbohydrates: proteins and lipids in the process of aggregation of natural marine organic matter investigated by means of 2D correlation spectroscopy applied to infrared spectra, *Spectrochim. Acta Part A* 71 (2009) 1877–1884.
- [65] J. Shang, J. Chen, Z. Shen, X. Xiao, H. Yang, Y. Wang, A. Ruan, Photochemical degradation of PAHs in estuarine surface water: effects of DOM salinity, and suspended particulate matter, *Environ. Sci. Pollut. Res.* 22 (2015) 12374–12383.
- [66] H. Xu, W.J. Cooper, J. Jung, W. Song, Photosensitized degradation of amoxicillin in natural organic matter isolate solutions, *Water Res.* 45 (2011) 632–638.
- [67] M.L. Dell’Arciprete, L. Santos-Juanes, A.A. Sanz, R. Vicente, A.M. Amat, J.P. Furlong, D.O. Mártire, M.C. Gonzalez, Reactivity of hydroxyl radicals with neonicotinoid insecticides: mechanism and chafes in toxicity, *Photochem. Photobiol. Sci.* 8 (2009) 1016–1023.
- [68] S. Carvalho, P. Pereira, F. Pereira, H. Pablo, C. Vale, M.B. Gaspar, Factors structuring temporal and spatial dynamics macrobenthic communities in a eutrophic coastal lagoon (Óbidos lagoon, Portugal), *Mar. Environ. Res.* 71 (2011) 97–110.
- [69] P. Pereira, H. Pablo, C. Vale, F. Rosa-Santos, R. Cesário, Metal and nutrient dynamics in a eutrophic coastal lagoon (Óbidos: Portugal): The importance of observations at different time scales, *Environ. Monit. Assess.* 158 (2009) 405–418.